

X-ray and Molecular Emission from the Nearest Region of Recent Star Formation

J. H. Kastner,* B. Zuckerman, D. A. Weintraub, T. Forveille

The isolated, young, sunlike star TW Hya and four other young stars in its vicinity are strong x-ray sources. Their similar x-ray and optical properties indicate that the stars make up a physical association that is on the order of 20 million years old and that lies between about 40 and 60 parsecs (between about 130 and 200 light years) from Earth. TW Hya itself displays circumstellar CO, HCN, CN, and HCO⁺ emission. These molecules probably orbit the star in a solar-system-sized disk viewed more or less face-on, whereas the star is likely viewed pole-on. Being at least three times closer to Earth than any well-studied region of star formation, the TW Hya Association serves as a test-bed for the study of x-ray emission from young stars and the formation of planetary systems around sunlike stars.

The nearest well-studied regions of the Milky Way galaxy that contain recently formed stars lie ~150 parsecs (pc) away in the Taurus (Tau), Ophiuchus (Oph), Lupus, and Chamaeleon (Cha) dark clouds. These clouds stretch over tens of parsecs and are composed mostly of cold hydrogen and helium gas. The gas is self-shielded from dissociating interstellar ultraviolet (UV) radiation, which allows the survival or formation (or both) of molecules and large dust grains. In regions where the density is high or the ionization fraction is low, pieces of these molecular clouds may collapse to form stars. Indeed, observations of dark clouds have enabled the identification of many hundreds of embedded and associated young, sunlike (T Tauri) stars. T Tauri stars are so young—a hundred thousand to a few million years old—that the process of core nuclear fusion, which powers the sun and all other stars for most of their lifetimes, is only just beginning. There is evidence from infrared (IR) and radio astronomy that many T Tauri stars possess circumstellar disks, which are potential sites of planet formation. Thus, T Tauri stars in and near molecular clouds are our main sources of information about the likely formative history of the sun and the planets.

In contrast, the T Tauri star TW Hya has earned notoriety on the basis of the absence of dark clouds in its general vicinity (1). It exhibits strong H α emission (as well as other optical emission lines) and Li ab-

sorption (1, 2), a combination that is characteristic of classical (as opposed to weak-lined) T Tauri stars (3). It has T Tauri-like excess continuum flux at near-IR and UV wavelengths (1) and is a strong submillimeter continuum source (4). But with no cloud identified that might have supplied the raw materials for its formation, the origin of TW Hya has been a puzzle to astronomers (5).

Optical spectroscopic surveys of field stars with excess far-IR emission (2, 6) identified four other stars located within 15° of TW Hya as isolated T Tauri stars (Table 1). Because these five stars are located in the same region of the sky and have similar radial velocities, it was suggested that they could be the remnant of a now-dissipated association (2, 6). In terms of the features of its optical-through-radio (7) spectrum, TW Hya remains the most extreme of the five. However, each of these stars displays H α emission (or H α absorption partially filled in by emission) or Li absorption (or both) (Table 1). H α equiv-

alent widths indicate that only TW Hya is clearly a classical T Tauri star; CoD -29° 8887 and HD 98800 are weak-lined T Tauri stars (8).

The T Tauri stars in Tau, Cha, and Oph have been the subject of many x-ray emission studies, including recent surveys conducted with the Roentgen satellite (ROSAT) (9–12). These studies indicate that most T Tauri stars are x-ray sources. Indeed, we determined that all five stars in Table 1 have x-ray counterparts in the ROSAT All-Sky Survey Bright Source Catalog (13) (Table 2). The means of the ROSAT count rates (C_x) and absorption-corrected fluxes (F_x) of these five stars exceed the mean C_x and F_x , respectively, of the optically identified cloud T Tauri stars by an order of magnitude or more (Table 3), which indicates that the isolated T Tauri stars (Table 1) are much closer to Earth than are the cloud T Tauri stars. The similar and large x-ray fluxes of the Table 1 stars support the evidence from radial velocities and optical spectra that these stars form a nearby physical association, henceforth referred to as the TW Hya Association.

For T Tauri stars associated with molecular clouds, the generally well-determined distances to the clouds provide estimates of the distances to the stars. These distances then enable astronomers to infer stellar luminosities and hence stellar ages, which are obtained from theoretical calculations of luminosity as a function of stellar mass and age. Because the TW Hya Association lacks an associated molecular cloud, one must employ other means to infer the distance and age of the TW Hya Association and thereby to situate its five members in pre-main sequence stellar evolution. Recent ROSAT surveys of T Tauri stars and young open clusters provide such a means (14–18). These surveys yielded measurements of the ratio of x-ray to bolometric luminosity

Table 1. Parameters for stars considered to be members of the TW Hya Association. RA and DEC are the right ascension and declination, respectively (J2000 coordinates), and m_v is the apparent visual magnitude. EW (H α) and EW(Li) are the equivalent widths of the H α and Li lines, respectively (2, 6, 32); we list EWs only for the brightest components of the multiple systems Hen(3) 600 and HD 98800 (a negative sign indicates H α in emission). D is the photometric distance, when one assumes that each star is 20 million years old (see text). The errors in D are estimates given uncertainties in stellar age (± 10 My) and mass (21, 22). Hen(3) 600 is a visual binary with separation 1.5"; D is derived with the assumption that the two components contribute equally to their combined m_v . HD 98800 is a quadruple system consisting of two spectroscopic binaries separated by 0.8" (32, 33); D is based on the measured flux ratio of the visual components, A:B = 1.3, and the spectral type of the primary. This flux ratio suggests a pre-main sequence system, since two main sequence stars with the (K5 and K7) spectral types of the Aa and Ba components of HD 98800 would have a larger flux ratio of 2.1.

Star	Spectral type	RA (J2000)	DEC (J2000)	m_v (mag)	EW(H α) (Å)	EW(Li) (Å)	D (pc)
TW Hya	K7 Ve	11 01 52.0	-34 42 16	11.1	-225	0.46	60 \pm 16
CoD -29° 8887	M0	11 09 13.9	-30 01 40	11.1	-2	0.52	48 \pm 12
Hen(3) 600	M3	11 10 27.9	-37 31 53	12.0	-20	0.55	39 \pm 7
HD 98800	K5 V	11 22 05.6	-24 46 38	8.9	(>-0.1)	0.43	49 \pm 9
CoD -33° 7795	M1	11 31 55.4	-34 36 25	11.4	-10	0.52	46 \pm 10

J. H. Kastner, Center for Space Research, Massachusetts Institute of Technology, 70 Vassar Street, Building 37-667a, Cambridge, MA 02139, USA.

B. Zuckerman, Department of Physics and Astronomy, University of California, Los Angeles, CA 90095, USA.

D. A. Weintraub, Department of Physics and Astronomy, Vanderbilt University, Post Office Box 1807 Station B, Nashville, TN 37235, USA.

T. Forveille, Groupe d'Astrophysique, Observatoire de Grenoble, 414 rue de la Piscine, F-38041 Grenoble Cedex, France.

*To whom correspondence should be addressed. E-mail: jhk@space.mit.edu

Table 2. ROSAT x-ray data for stars of the TW Hya Association. The designation "1RXP" in the ROSAT name refers to pointed observations, whereas "1RXS" refers to ROSAT All-Sky Survey observations. σ is the position uncertainty of the ROSAT x-ray source, Δ is the offset between the ROSAT x-ray source position and the optical position of the star and C_x is the ROSAT Position Sensitive Proportional Counter (PSPC) count rate. For TW Hya and Hen(3) 600, the differences in C_x for pointed and survey data likely are be-

cause of variability in the x-ray fluxes of these stars. F_x is the x-ray flux estimated from the ROSAT PSPC count rate (9). For all stars except TW Hya, we neglect absorption in converting from count rates to fluxes; for TW Hya we assume an absorbing column density of $1.2 \times 10^{20} \text{ cm}^{-2}$, on the basis of a fit to its pointed PSPC spectrum (34). L_x/L_{bol} is the ratio of x-ray luminosity to bolometric luminosity. For TW Hya and Hen 600, one value of $\log(L_x/L_{\text{bol}})$ is listed, which uses the mean of the results for F_x as derived for pointed and survey x-ray data.

Star	ROSAT name	σ (arc sec)	Δ (arc sec)	C_x (s^{-1})	F_x ($\text{ergs cm}^{-2} \text{ s}^{-1}$)	$\log(L_x/L_{\text{bol}})$
TW Hya	1RXP J110152-3442.2	12	4	0.310 ± 0.007	2.4×10^{-12}	-3.05
	1RXS J110152.0-344212	7	4	0.57 ± 0.04	4.5×10^{-12}	
CoD -29° 8887	1RXS J110913.5-300133	8	8	0.34 ± 0.03	2.6×10^{-12}	-3.08
Hen(3) 600	1RXP J111028-3731.8	7	5	0.154 ± 0.003	1.2×10^{-12}	-3.21
	1RXS J111028.9-373204	10	16	0.28 ± 0.03	2.2×10^{-12}	
HD 98800	1RXS J112205.4-244632	7	6	0.66 ± 0.05	5.2×10^{-12}	-3.43
CoD -33° 7795	1RXS J113155.7-343632	8	6	0.66 ± 0.08	5.2×10^{-12}	-2.74

(L_x/L_{bol} , where L_{bol} is the luminosity of a star integrated over all wavelengths) for large numbers of low-mass stars. The ratio L_x/L_{bol} is independent of distance and, provided that the x-ray emission is coronal in origin, is diagnostic of stellar activity and hence age (19) (Fig. 1).

Qualitatively, the large ratios of $\log(L_x/L_{\text{bol}})$ measured for the TW Hya Association stars indicate that they are highly evolved T Tauri stars. Specifically, the mean $\log(L_x/L_{\text{bol}})$ of the five known

members of the TW Hya Association, -3.10 ± 0.11 (Table 2), suggests an age of at least ~ 20 million years (My) (Fig. 1). Hence TW Hya could well be the oldest known classical T Tauri star (9, 10). This age estimate is quite uncertain given the small known membership of the association and the likelihood that their x-ray fluxes are variable. Furthermore, all of the stars in the association show strong Li absorption (Table

1), which suggests that the age of the association may be less than 20 My (20). Even if the TW Hya Association is as young as 10 My, which appears unlikely given the large mean value of $\log(L_x/L_{\text{bol}})$ for the association, its stars would be within a factor of 4 or so of their main sequence luminosities, based on theoretical models of pre-main sequence stellar evolution (21, 22). Hence, from the plausible age range of the association, we ascertain that its five known members lie between 39 and 60 pc from Earth (Table 1) (23). This confirms the prior inference, based on the high galactic latitudes of these stars, that they are relatively nearby (2). At a mean distance of 48 pc, the linear extent of the association in the plane of the sky is ~ 10 pc, which is similar to its line-of-sight distance dispersion (Table 1) and similar in size to typical star-forming clouds. We conclude that the TW Hya Association likely constitutes the nearest region of recent star formation. Its only rival in terms of proximity to Earth may be the handful of stars embedded in the small high-latitude cloud MBM 12, which is estimated to be 65 pc from Earth (24). Indeed, the small cluster in MBM 12 may resemble the TW Hya Association at an early epoch, before molecular cloud dispersal.

Given its proximity and age and the absence of the confusing signatures of a host molecular cloud, observations of the TW Hya Association and TW Hya in particular could yield insight into the process of planet formation. The substantial IR and sub-millimeter emission from TW Hya is indicative of substantial quantities of orbiting particulate matter. Hence TW Hya may be undergoing or perhaps has recently ended a period of giant planet building. Given the large distance of TW Hya from known molecular clouds, the localization of CO emission at the position of the star, and the narrow CO line widths, Zuckerman *et al.* (7) concluded that TW Hya is orbited by a

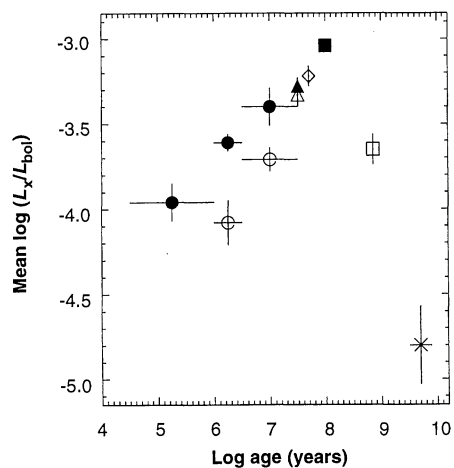


Fig. 1. Mean of the log of the ratio of the x-ray to bolometric luminosity for dwarf stars in the range of spectral types corresponding to that of the TW Hya Association, K5 to M3. We include only clusters for which 60 to 80% of K and M stars have identified x-ray counterparts [accounting for x-ray nondetections would move all points downward by 0.1 to 0.2 in $\log(L_x/L_{\text{bol}})$]. Data for T Tauri stars are from surveys of Taurus-Auriga (9) (filled circles) and Cha (10) (open circles). Data for young open cluster stars are from surveys of IC 2602 (15) (filled triangle), IC 2391 (17) (open triangle), α Per (16) (diamond), the Pleiades (14) (filled square), and the Hyades (18) (open square). Also shown is the $\log(L_x/L_{\text{bol}})$ for an older field star sample (38) (cross). The mean of the Table 1 stars, $\log(L_x/L_{\text{bol}}) = -3.10 \pm 0.11$, suggests a median age of at least 20 My.

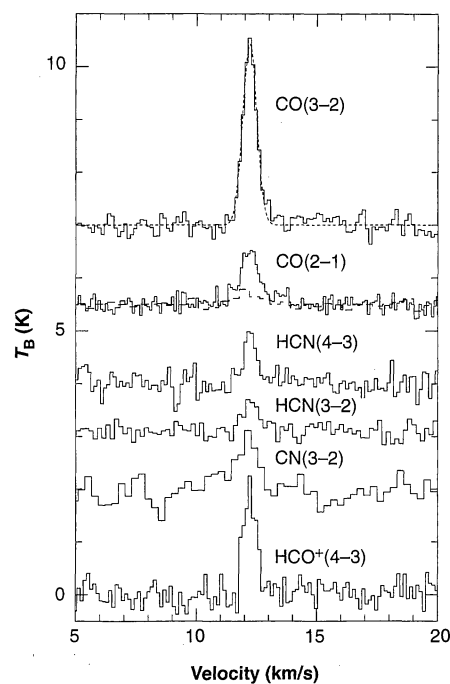


Fig. 2. Molecular spectra observed toward TW Hya with the JCMT. The abscissa is the heliocentric radial velocity, and the ordinate is the relative main-beam brightness temperature T_B . The short dashed curve overlaying the CO(3-2) line profile represents the best-fit Gaussian function (Table 4). The two spectra labeled CO(2-1) are of the ^{12}CO (solid curve) and ^{13}CO (dashed curve) isotopomers (the ^{13}CO spectrum has been expanded along the ordinate by a factor of 2). For clarity, the only CN(3-2) line shown is the brightest detected hyperfine component (at 340.2478 GHz).

nearly face-on molecular cloud of roughly solar-system dimensions. This disk may well resemble the early solar nebula, especially given the apparent lack of a binary companion to TW Hya (25).

To probe its circumstellar chemistry and physics, we obtained spectra of TW Hya at a number of rotational transitions of CO, ¹³CO, and other molecular species commonly observed in interstellar clouds and in the circumstellar envelopes of evolved stars. These submillimeter line data were obtained with the 15-m James Clerk Maxwell Telescope (JCMT) on Mauna Kea, Hawaii, in June 1995, February 1996, and November 1996 (26). In addition to CO and ¹³CO, which we detected at higher rotational transitions than had been observed previously (7), we detected transitions of HCN, CN, and HCO⁺ toward TW Hya (Table 4). We failed to detect CS, H₂CO, H¹³CN, and HNC. The measured ¹²CO(2–1):¹³CO(2–1) line ratio, ~7, is an order of magnitude less than the solar system abundance ratio of ¹²C:¹³C, which indicates that the CO emission is optically thick. Gaussian functions fitted to the line profiles have full widths at half maximum (FWHM) of ΔV ~ 0.7 km s⁻¹ for the detected transitions (Table 4). Notably, the CO profiles are well described as Gaussian and do not display the broad wings typical of bipolar molecular outflows from young low-mass stars (Fig. 2). It would be surprising to detect such an outflow signature, given the absence of cloud CO emission surrounding TW Hya; that is, there exists no ambient molecular gas to be swept up by a bipolar stellar wind, if present. Hence, the detected molecular gas is bound to the star.

The relative intensities of the optically thick (2–1), (3–2), and (4–3) transitions of CO constrain the excitation conditions in the emitting region. The measured intensity is proportional to the fraction of the telescope beam that is subtended by the emitting region, so if the radius of this region is the same in all three transitions, then the line intensities scale inversely with beam area. The measured ratios of (2–1):(3–2):(4–3) emission (1.0:1.9:5) equal, within measurement uncertainty, the ratios of inverse beam areas (1.0:1.9:3.3); hence the CO gas is well excited throughout the emitting region. Because the upper level of the (4–3) transition is 55 K above ground, the bulk of the molecular gas must be at temperatures ≥50 K. A similar result is obtained from the ratio of the observed HCN lines, although the ratio of the (3–2) to (4–3) HCN line intensities (1.0:1.2) is somewhat larger than the ratio of the inverse beam areas (1.0:1.7). If TW Hya is 60 pc from Earth, the measured ¹³CO(2–1) line

intensity suggests a molecular (H₂) mass of ~7 × 10²⁸ g, or 11 Earth masses (27).

On the basis of the measured intensity of optically thick ¹²CO(2–1) (Table 1), the JCMT beam size at 230 GHz (20"), and the inferred gas kinetic temperature (≥50 K), we estimated an emitting region radius of

~1", or R_{CO} ~ 60 astronomical units. At this radius, the Keplerian orbital velocity of a particle around a ~0.7 solar mass star (the approximate mass of TW Hya if its age is 20 My) is ~3 km s⁻¹, which is an order of magnitude larger than the measured half widths of the molecular emission lines (Ta-

Table 3. Mean x-ray count rates and fluxes of T Tauri star associations. *N* is the number of stars in each association that have spectral types in the range of the TW Hya Association (K5 to M3) (35); the listed mean values of log C_x and log F_x are calculated for these subsamples only. For Taurus and Chamaeleon stars, values of F_x are determined by authors (9, 10) from ROSAT count rates corrected for inferred x-ray extinction and then converted to x-ray luminosities with the assumption of a distance of 140 pc to each cloud. Here we have converted L_x back to F_x on the basis of this assumed distance. Mean log F_x values for Tau and Cha have not been corrected for sample incompleteness; accounting for x-ray nondetections will diminish ⟨log F_x⟩ by not more than 0.2 for each sample (9).

Association	<i>N</i>	⟨log C _x ⟩	⟨log F _x ⟩	Reference
TW Hya	5	-0.4 (0.1)	-11.5 (0.1)	Table 2
Taurus	28	-1.59 (0.05)	-12.60 (0.05)	(9)
Chamaeleon	35	-2.16 (0.07)	-13.06 (0.07)	(10, 12)

Table 4. Molecular species observed toward TW Hya. *ν* is the frequency of the rotational transition, ∫ T_B d*V* is the integrated line intensity, V_☉ is the central velocity of the line in the heliocentric frame, Δ*V* is the FWHM, and T_B is the peak line brightness temperature. The listed upper limits are at the 3σ confidence level. Line parameters for CN are based on a simultaneous fit to all hyperfine features; securely detected components lie at the listed frequencies. The results of this fit imply the CN emission is optically thin, when one assumes that there is LTE within the hyperfine multiplet. Dashes indicate undetermined line parameters.

Molecule	Transition	<i>ν</i> (GHz)	∫ T _B d <i>V</i> (K km s ⁻¹)	V _☉ (km s ⁻¹)	Δ <i>V</i> (km s ⁻¹)	T _B (K)
CO	2–1	230.5380	1.02 (0.05)	12.21 (0.03)	0.70 (0.08)	0.95 (0.1)
	3–2	345.7960	1.91 (0.06)	12.21 (0.01)	0.69 (0.02)	2.6 (0.1)
	4–3	461.0408	5 (1)	12.3*	0.6*	9 (4)
¹³ CO	2–1	220.3987	0.14 (0.05)	12.0 (0.1)	0.9 (0.4)	0.14 (0.06)
	3–2	330.5800	–	12*	–	0.3*
HCN	3–2	265.8864	0.45 (0.07)	12.26 (0.06)	0.76 (0.15)	0.56 (0.06)
	4–3	354.5055	0.53 (0.09)	12.23 (0.04)	0.52 (0.09)	0.96 (0.06)
H ¹³ CN	4–3	345.3398	–	–	–	<0.6
HNC	4–3	362.6299	–	–	–	<1.2
CN	3–2	340.0315	0.4 (0.15)	12.20 (0.04)	0.69 (0.10)	0.5 (0.2)
		340.0354	0.4 (0.15)	12.20 (0.04)	0.69 (0.10)	0.5 (0.2)
		340.2478	1.2 (0.2)	12.20 (0.04)	0.69 (0.10)	1.6 (0.3)
CS	7–6	342.883	–	–	–	<0.9
HCO ⁺	4–3	356.73425	1.4 (0.1)	12.22 (0.02)	0.62 (0.04)	2.0 (0.2)
H ₂ CO	3 ₁₂ –2 ₁₁	225.6978	–	–	–	<0.5
		5 ₁₅ –4 ₁₄	351.7687	–	–	–

*Tentative results.

Table 5. Circumstellar molecular abundances for TW Hya (36), the T Tauri star DM Tau (37), and planetary nebulae (PNe) (30). X/¹³CO is the abundance relative to ¹³CO (abundance relative to H₂ will be a factor ~10⁻⁶ smaller, when one assumes the terrestrial ¹³C to ¹²C abundance ratio of 89 and a ¹²CO abundance of ~10⁻⁴ relative to H₂), and X/HCN is the abundance relative to HCN. Means and standard deviations for PNe exclude NGC 7027. Dashes indicate that data are unavailable.

Molecule	TW Hya		DM Tau		PNe X/HCN
	X/ ¹³ CO	X/HCN	X/ ¹³ CO	X/HCN	
HCN	0.005	(1)	0.002	(1)	(1)
CN	0.04	8	0.010	5	9 ± 3
HCO ⁺	0.012	2.4	0.002	1.3	0.5 ± 0.2
HNC	<0.009	<0.6	0.0008	0.4	0.4 ± 0.2
CS	<0.02	<1.3	0.001	0.6	<0.08
H ₂ CO	<0.012	<0.8	0.002	1.0	–
H ¹³ CN	<0.012	<0.8	–	–	–

ble 4). Thus, if the emission arises in a rotating circumstellar disk, then the combination of the compact emitting region and the narrow line profiles indicates that we view this disk nearly along its polar axis. Indeed, the intensities, widths, and (single-peaked) shapes of the observed CO lines resemble those predicted for compact, face-on molecular disks (28). A face-on orientation is also indicated by the combination of small visual extinction (1) and large IR and submillimeter excess (4, 29). The projected rotational velocity ($v \sin i \approx 15 \text{ km s}^{-1}$) and inferred rotation period of TW Hya (1.3 days) also suggest that we view the star itself pole-on (7). This conclusion is supported by the observation that most young stars that are as x-ray luminous as TW Hya have projected rotational velocities $v \sin i > 15 \text{ km s}^{-1}$ (14).

The circumstellar abundances of HCN, CN, and HCO^+ are very similar to those determined for DM Tau, a classical T Tauri star (Table 5). For both stars, the relative abundances of CN and HCN resemble those of molecule-rich planetary nebulae (Table 5). A planetary nebula is one of the last stages of evolution of a solar-mass star that has ejected and subsequently ionized its former envelope. Because the molecular chemistry (in particular, the large CN/HCN abundance ratio and large HCO^+ abundance) of a planetary nebula is engendered by ionizing UV and, possibly, x-ray flux from the newly unveiled white dwarf at its core (30), it follows that the circumstellar environment of TW Hya may be similarly photon-dominated. This is not particularly surprising given the substantial UV excess (1) and x-ray flux (Table 2) that characterize TW Hya. Thus it is likely that the intense radiation field of TW Hya has changed the molecular composition of the circumstellar gas from that of the cloud that spawned it. Furthermore, x-ray or UV photon heating (or both) may be more important to the overall energy balance of the observed molecular gas than is dust-gas collisional heating. If the circumstellar molecular chemistry is photon-dominated, models of molecular line emission from protoplanetary disks would need to be revised, because such models typically assume that gas-dust collisions dominate gas heating (31).

REFERENCES AND NOTES

- S. M. Rucinski and J. Krautter, *Astron. Astrophys.* **121**, 217 (1983).
- R. de la Reza, C. A. O. Torres, G. Quast, B. V. Castilho, G. L. Vieira, *Astrophys. J.* **343**, L61 (1989).
- The combination of $\text{H}\alpha$ emission and strong Li absorption indicates stellar youth and is commonly used to identify T Tauri stars. The strength of the $\text{H}\alpha$ emission serves to classify such stars either as classical (commonly defined as a T Tauri star with an $\text{H}\alpha$ emission equivalent width of $\geq 10 \text{ \AA}$) or weak-lined.
- D. A. Weintraub, G. Sandell, W. Duncan, *Astrophys. J.* **340**, L69 (1989).
- E. D. Feigelson, *ibid.* **468**, 306 (1996).
- J. Gregorio-Hetem, J. R. D. Lepine, C. A. O. Torres, R. de la Reza, *Astron. J.* **103**, 549 (1992).
- B. Zuckerman, T. Forveille, J. H. Kastner, *Nature* **373**, 494 (1995).
- Hen(3) 600 and CoD -33° 7795 might be considered classical T Tauri stars on the basis of $\text{H}\alpha$ emission alone. However, some authors also use the presence of excess near-IR emission to discriminate between classical and weak-lined T Tauri stars. Extrapolating from existing photometry, we anticipate that CoD -33° 7795 does not have a near-IR excess and therefore is likely to be better classified as weak-lined. The near-IR flux of Hen 600 is more difficult to predict, and its status (weak-lined versus classical) remains uncertain.
- R. Neuhaeuser, M. F. Sterzik, J. H. M. M. Schmitt, R. Wichmann, J. Krautter, *Astron. Astrophys.* **297**, 391 (1995).
- W. A. Lawson, E. D. Feigelson, D. P. Huenemoerder, *Mon. Not. R. Astron. Soc.* **280**, 1071 (1996).
- S. Casanova, T. Montmerle, E. D. Feigelson, P. André, *Astrophys. J.* **439**, 752 (1995).
- E. D. Feigelson, S. Casanova, T. Montmerle, J. Guibert, *ibid.* **416**, 623 (1993).
- W. Voges *et al.*, *Astron. Astrophys.*, in press.
- J. R. Stauffer, J.-P. Caillault, M. Gagné, C. F. Prosser, L. W. Hartmann, *Astrophys. J. Suppl. Ser.* **91**, 625 (1994).
- S. Randich, J. H. M. M. Schmitt, C. F. Prosser, J. R. Stauffer, *Astron. Astrophys.* **300**, 134 (1995).
- , *ibid.* **305**, 785 (1996).
- B. M. Patten and T. S. Simon, *Astrophys. J. Suppl. Ser.* **106**, 489 (1996).
- J. P. Pye, S. T. Hodgkin, R. A. Stern, J. R. Stauffer, *Mon. Not. R. Astron. Soc.* **266**, 798 (1994).
- Low-mass stars possess deep convective envelopes. Such deep convective zones, in combination with fast rotation, have been shown empirically to be conducive to chromospheric activity and coronal x-ray emission [D. S. Hall, in *The Sun and Cool Stars: Activity, Magnetism, and Dynamos*, I. Tuominen, D. Moss, A. Rudiger, Eds. (IAU Colloquium No. 130, Springer-Verlag, Berlin, 1991), pp. 353–369]. Over much of its pre-main sequence and early main sequence evolution (that is, up to an age of $\sim 100 \text{ My}$), a low-mass star is continually contracting. Contraction has two observable consequences: a steady decrease in bolometric luminosity and a steady increase in rotation rate (once a circumstellar disk dissipates), attributable to conservation of angular momentum. Its increasing rate of rotation, combined with ongoing deep convection, ensures that a low-mass star's magnetic activity is maintained for the first $\sim 100 \text{ My}$ of its life. This inference is supported by the observation that the mean x-ray luminosity of low-mass stars remains approximately constant from late pre-main sequence through early main sequence stages [C. Briceño *et al.*, *Astron. J.* **113**, 740 (1997)] and by the correlation between the rotation rate and $\log(L_x/L_{\text{bol}})$ for Pleiades members (14). Thus, with L_x remaining roughly constant and L_{bol} steadily declining for low-mass ($\leq 0.7 M_\odot$) stars over their first $\sim 100 \text{ My}$ of evolution (21, 22), the net result is the observed steady increase in L_x/L_{bol} over the same period (Fig. 1). By the time a low-mass star nears the main sequence (that is, by Pleiades age), its relative x-ray luminosity is near the empirical "saturation" level of $\log(L_x/L_{\text{bol}}) \sim -3$ (14). This would appear to represent the maximum efficiency with which dynamo activity (resulting from the combination of fast rotation and deep convection) can convert a star's luminosity to coronal x-ray emission. Subsequently, single low-mass stars gradually spin down and become less active; by the time such stars are as old as the sun, they are relatively meager x-ray emitters.
- The presence and strength of Li absorption in the spectrum of a young star are useful, but controversial age indicators [see discussion in (32)]. Models predict that Li should be fully depleted in stars of the mass of TW Hya by $\sim 10 \text{ My}$ (22); however, substantial abundances of Li are present in low-mass stars that are as old as 30 to 100 My [J. R. Stauffer *et al.*, *Astrophys. J.* **479**, 776 (1997); M. Zboril *et al.*, *Mon. Not. R. Astron. Soc.* **284**, 685 (1997)].
- S. Stahler, personal communication.
- F. D'Antona and I. Mazzitelli, *Astrophys. J. Suppl. Ser.* **90**, 467 (1994).
- After this paper was accepted, we became aware of the Hipparcos satellite parallax measurements of the distances to TW Hya, $56 \pm 7 \text{ pc}$ (R. Wichmann, U. Bastian, J. Krautter, I. Jankovics, S. M. Rucinski, paper presented at the Hipparcos Venice '97 Symposium, Venice, Italy, 13 to 16 May 1997), and HD98800, $47 \pm 6 \text{ pc}$ [from data available in the Hipparcos catalog (<http://vizier.u-strasbg.fr/cgi-bin/VizieR>) as of 17 June 1997]. These distances agree with our estimates (Table 1) and confirm our earlier conclusions.
- L. Magnani, J.-P. Caillault, A. Buchalter, C. A. Beichmann, *Astrophys. J. Suppl. Ser.* **96**, 1 (1995).
- A. Ghez, personal communication.
- We used receivers A2, B3i, and C2 for measurements in the 230-, 345-, and 460-GHz atmospheric windows. Beam sizes at these frequencies were 20", 14", and 11", respectively. The back end was the JCMT Digital Autocorrelation Spectrometer (DAS); we used a DAS bandwidth of 250 MHz, which yields a spectral resolution of 189 kHz. We obtained data by switching the secondary mirror at 1 Hz between the position of TW Hya and a nearby reference position located 60" away (40" away, for observations at 460 GHz). Typical total integration times were on the order of 1 hour. To convert from antenna temperatures to brightness temperatures, we applied aperture efficiencies of 0.57, 0.49, and 0.31 for observations in the 230-, 345-, and 460-GHz windows, respectively.
- For the calculation of circumstellar molecular mass, we assumed a gas phase CO abundance typical of interstellar molecular clouds ($\text{CO}/\text{H}_2 \sim 10^{-4}$ by number). If CO were severely depleted, then we would underestimate the circumstellar H_2 mass. Temperatures $\geq 50 \text{ K}$ are too high for substantial CO ice mantles to form on dust grains, however, so any missing CO likely is trapped in small planetesimals or in planets rather than frozen out into grains. The measured line ratios likewise preclude a large mass of "missing" gas at low temperature. The inferred H_2 mass and emitting region radius suggest an average H_2 density $\sim 5 \times 10^7 \text{ cm}^{-3}$ (approximating the emitting region as a cylinder of radius R_{CO} and height $0.2R_{\text{CO}}$). Such a density is sufficient to excite the (3–2) and (4–3) transitions of HCN [R. Genzel, in *Millimeter and Submillimeter Astronomy*, R. D. Wolstencroft and W. B. Burton, Eds. (Kluwer, Norwell, MA, 1987), p. 223].
- S. V. W. Beckwith and A. I. Sargent, *Astrophys. J.* **402**, 280 (1993); T. Omodaka, Y. Kitamura, E. Kawazoe, *ibid.* **396**, L87 (1992).
- S. Rucinski, *Astron. J.* **90**, 2321 (1985).
- P. Cox, A. Omont, P. J. Huggins, R. Bachiller, T. Forveille, *Astron. Astrophys.* **266**, 420 (1992); R. Bachiller, T. Forveille, P. J. Huggins, P. Cox, *ibid.*, in press.
- S. V. W. Beckwith, A. I. Sargent, R. S. Chini, R. Gusten, *Astron. J.* **99**, 924 (1990).
- D. R. Soderblom, T. J. Henry, M. D. Shetrone, B. F. Jones, S. H. Saar, *Astrophys. J.* **460**, 984 (1996).
- G. Torres, R. P. Stefanik, D. W. Latham, T. Mazeh, *ibid.* **452**, 870 (1995).
- J. H. Kastner, unpublished data.
- Our criteria for selecting stars in the range of spectral types K5 to M3 were published spectral type or stellar effective temperature or B–V and V–I colors (or both) (where we adopted ranges of B–V between 1.1 and 1.6 and V–I between 1.6 and 2.9).
- The circumstellar molecular abundances for TW Hya were calculated assuming local thermodynamic equilibrium (LTE), optically thin emission, and a uniform excitation temperature of $T_{\text{ex}} \sim 50 \text{ K}$. The last approximation can be valid only in the outermost portion of the emitting region. However, because abundances were calculated relative to ^{13}CO and because the partition functions for all of these species (including ^{13}CO) scale more or less linearly with T_{ex} over a wide range of gas temperatures (from $\sim 10 \text{ K}$ to over 300 K), the relative abundance estimates do not depend on the detailed radial distribution of T_{ex} .
- A. Dutrey, S. Guilloteau, M. Guélin, *Astron. Astro-*

- phys. Lett.* **317**, L55 (1997).
38. T. A. Fleming, J. H. M. M. Schmitt, M. A. Giampapa, *Astrophys. J.* **450**, 401 (1995).
39. J.H.K.'s research at the Massachusetts Institute of Technology was supported in part by the Advanced X-ray Astrophysics Facility Science Center as part of Smithsonian Astrophysical Observatory contract

SVI-61010 under the NASA Marshall Space Flight Center. Additional support was provided by NASA Origins of Solar Systems program grants (NAGW 5020 and 5145) to Vanderbilt University (D.A.W.) and by an NSF grant (AST-9417158) to the University of California, Los Angeles (B.Z.). We thank E. J. Gaidos (M.I.T.) and H. Matthews (Joint Astronomy Centre),

who assisted in the molecular line observations, and T. S. Simon, who provided data before publication. Our molecular abundance calculations made use of the Jet Propulsion Laboratory's online Molecular Spectroscopy database.

28 January 1997; accepted 7 May 1997

Early Humans and Rapidly Changing Holocene Sea Levels in the Queen Charlotte Islands–Hecate Strait, British Columbia, Canada

Heiner Josenhans,* Daryl Fedje, Reinhard Pienitz, John Southon

Marine cores from the continental shelf edge of British Columbia (Canada) demonstrate that sea level at the shelf edge was 153 meters below present 14,000 calendar years ago and more than 30 meters lower than the maximum eustatic low of –120 meters. Dated artifacts, including stone tools, indicate that humans occupied this region by at least 10,200 calendar years before present (B.P.). Local sea level rose rapidly (5 centimeters per year) during the period of early human occupation as a result of eustatic sea-level rise and glacio-isostatic forebulge movement. This shelf edge site was first elevated and then subsided. The exposed shelf edge was available for human occupation and may have served as a migration route during times of lowered sea levels between 13,500 and 9500 ^{14}C years B.P.

The continental shelf of British Columbia and the coastal fjord embayments reveal evidence of postglacial sea level that changed rapidly about 14,000 years ago (1–4). Contemporaneous but regionally tilted paleoshorelines are documented at elevations from +200 m (5) at the head of Kitimat Fiord (Fig. 1) to –140 m at the continental shelf edge, a distance of 200 km.

Mapping the paleoenvironments and locating early human remains along these inferred paleocoastlines is of special interest with respect to extending the possible human migration routes to North America beyond those recently reported (6) in the Bering Strait. Here we combine data from seismic reflection mapping and piston coring in the offshore with archaeological, faunal, floral, and ^{14}C analysis to reconstruct the postglacial sea-level history and paleoenvironments of the Gwaii Haanas (7) region of the Queen Charlotte Island archipelago (Figs. 1 and 2) and specifically Juan Perez Sound.

To establish the age and elevation of paleoshorelines, we identified and cored formerly subaerial basins (Fig. 2) with sills

at different elevations and dated the paleocontacts between freshwater and marine sediments (8, 9). In the study area, numerous isolated basins formed during glaciation with sills at different elevations. The transition from freshwater basinal sedimentation to marine deposition was determined by analysis of diatoms from core samples. The age of the marine inundation was determined mostly from ^{14}C -dated wood fragments. We preferentially dated twigs and cones to avoid errors introduced by ancestral wood. Sill depth was obtained from hydrographic field sheet data, published charts, and sounding data obtained along seismic profiles (Fig. 3). Seismic reflection data collected across the sills were used to determine their composition and relative age. Bathymetric data were merged with terrestrial elevation data (1:20,000) to develop a digital terrain model around the Queen Charlotte Islands (10).

Five isolation basins within a 50-km radius (Fig. 2) were located by high-resolution seismic profiling and sidescan sonar. These were sampled by piston or vibracore (4). We also cored and dated several lakes near the coast to define the maximum elevation of raised shorelines (11). In Juan Perez Sound (Fig. 3), a submerged delta (depth = 153 m) and paleoriver system are evident in seismic data; we sampled these with a vibracore to establish the time of marine transgression. We obtained 267 radiocarbon dates (12, 13). The data set consists of 86 dates on archaeological sites, 52 dated

raised paleobeach deposits, 30 from lake cores, and 99 from marine cores. Dates on 72 shell-wood pairs indicate a marine reservoir correction of 600 years for shell dates (12, 14).

Changes in the ^{14}C production rate or disturbances in the carbon cycle during deglaciation, or both, have affected radiocarbon levels in the atmosphere and produced substantial age plateaus at ^{14}C ages of 9600, 10,000, and 10,500 ^{14}C years before present (B.P.) (15–17). We used dendrochronological and U-Th radiocarbon calibrations (16, 18–21), plus additional data from European lake sediment records (15, 17), to convert the ^{14}C ages to calendar ages.

The data show that sea level varied from –153 to +16 m between 14,600 and 10,100 calendar years B.P. (Fig. 4 and Table 1). Drowned isolation basins with sills at –107, –80, –45, and +16 m define four of the sea-level curve points. For example, marine incursion of the fjord embayment of Logan Inlet, which has a sill height of –80 m (site 4, Fig. 2, and Fig. 3, left), occurred 12,300 calendar years B.P. Diatom analysis indicated that marine incursion is marked by the transition from a freshwater diatom assemblage including *Tabellaria fenestrata*,

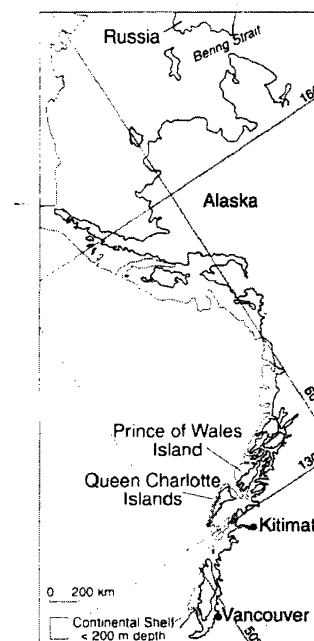


Fig. 1. Index map of the study area showing continental shelf areas shallower than –200 m that may have served as a coastal migration corridor during times of low sea level.

H. Josenhans, Geological Survey of Canada (Atlantic), Dartmouth, Nova Scotia B2Y 4A2, Canada.

D. Fedje, Canadian Heritage, Parks Canada, Victoria, British Columbia V8W 2G5, Canada.

R. Pienitz, Department of Geography, Université Laval, Quebec City, Quebec G1K 7P4, Canada.

J. Southon, University of California, Lawrence Livermore National Laboratory, CA, 94551–9900, USA.

*To whom correspondence should be addressed. E-mail: Josenhan@agc.bio.nsl.ca